Generating photoacoustic signals using high-peak power pulsed laser diodes.

Thomas J. Allen, B. T. Cox and Paul C. Beard

Department of Medical Physics and Bioengineering, Malet Place Engineering Building, Gower Street, London, UK;

ABSTRACT

Photoacoustic signals are usually generated using bulky and expensive Q-switched Nd:YAG lasers, with limited scope for varying the pulse repetition frequency, wavelength and pulse width. An alternative would be to use laser diodes as excitation sources; these devices are compact, relatively inexpensive, and available in a wide variety of NIR wavelengths. Their pulse duration and repetition rates can also be varied arbitrarily enabling a wide range of time and frequency domain excitation methods to be employed. The main difficulty to overcome when using laser diodes for pulsed photoacoustic excitation is their low peak power compared to Q-switched lasers. However, the much higher repetition rate of laser diodes ($\sim$ kHz) compared to many Q-switched laser systems ($\sim$ tens of Hz) enables a correspondingly greater number of events to be acquired and signal averaged over a fixed time period. This offers the prospect of significantly increasing the signal-to-noise ratio (SNR) of the detected photoacoustic signal. Choosing the wavelength of the laser diode to be lower than that of the water absorption peak at 940nm, may also provide a significant advantage over a system lasing at 1064nm for measurements in tissue. If the output of a number of laser diodes is combined it then becomes possible, in principle, to obtain a SNR approaching that achievable with a Q-switched laser. It is also suggested that optimising the pulse duration of the laser diode may reduce the effects of frequency-dependent acoustic attenuation in tissue on the photoacoustic signal. To investigate this, a numerical model based on the Poisson solution to the wave equation was developed. To validate the model, a high peak power pulsed laser diode system was built. It was composed of a 905nm stacked array laser diode coupled to an optical fibre and driven by a high current laser diode driver. Measurements of the SNR of photoacoustic signals generated in a purely absorbing medium (ink) were made as a function of pulse duration. This preliminary study shows the potential for using laser diodes as excitation sources for photoacoustic applications in the biomedical field.

Keywords: Laser diodes, Photoacoustics

1. INTRODUCTION

Photoacoustic signals are usually generated using Q-Switched lasers; these devices have the advantages of delivering high peak power pulses with ns pulse durations. However, it is difficult to make spectroscopic measurements with such lasers as they are available in a limited range of suitable wavelengths. An alternative would be to use laser diodes[1–3] as excitation sources as they are available in a wide range of visible and NIR wavelengths. Combining as few as three different wavelengths would allow for physiological monitoring of oxy and deoxy-haemoglobin.[4] Laser diodes also provide other advantages such as high repetition rate and variable pulse duration, enabling a wide range of time and frequency domain excitation methods to be employed. They are also compact and reasonably inexpensive. The main disadvantage of laser diodes is their low peak power which limits the rate at which sufficient optical energy can be delivered to the medium, thus limiting the efficiency of the photoacoustic generation process. In this study, we explore the possibility of overcoming this by (1) optimising the pulse duration to reduce the effects of acoustic attenuation, (2) exploiting the high pulse repetition rate of laser diodes to rapidly signal average over many aquisitions, (3) taking advantage of the shorter wavelengths (<905nm) of NIR laser diodes to mitigate the effect of optical attenuation due to water absorption in tissue.

Section 2 describes an analytical and numerical model used to simulate photoacoutic signals for different pulse durations. The numerical model is validated in section 3 by comparing the simulated signals to experimental

Send correspondence to T. J. Allen E-mail: tjallen@medphys.ucl.ac.uk,

Proc. SPIE **5696**, pp 233-242, 2005
SPIE BIOS 2005, 23-25 January 2005, San Jose, USA

data. A study of the effects of varying the pulse duration on the photoacoustic signal is described in section 4 using the numerical model. Section 5 and section 6 discuss possibilities to improve the photoacoustic SNR, firstly by signal averaging and secondly by considering optical attenuation in tissue at NIR wavelength.

2. THEORY

This section describes the analytical and numerical model used to simulate the effect of pulse duration on the photoacoustic signal.

2.1. Analytical model

When collimated light is incident on a pure absorber its intensity will decrease exponentially due to the absorption of the medium, this follows the Lambert-Bouguer law.

$$F(z) = F_0 e^{-\mu_a z} \tag{1}$$

Where $F(z)$ is the fluence at depth z, F_0 is the fluence at the surface and μ_a is the absorption coefficient of the pure absorber.

The absorbed light will create a temperature rise in the medium causing it to expand. This increase in volume is proportional to the change in temperature θ, and can be expressed by

$$\Delta v = \beta \theta v \tag{2}$$

where β is the thermal expansion coefficient of the medium and v the initial volume of the heated region.

The expansion will cause strain in the heated volume, consequently generating stress which will excite pressure waves. The initial pressure p_o is,

$$p_0 = B\frac{\Delta v}{v} \tag{3}$$

where B is the isothermal bulk modulus.

Using equation 2 and 3 it is possible to express the pressure as a function of temperature increase.

$$p_0 = B\beta\theta \tag{4}$$

Where θ is directly proportional to the energy deposited in the medium.

$$\theta = \frac{1}{C\rho} F_0 \mu_a e^{-\mu_a z} \tag{5}$$

Where C is the specific heat at constant volume.

Introducing equation 5 into 4 gives:

$$p_0(z) = \frac{B\beta}{C\rho} F_0 \mu_a e^{-\mu_a z} \tag{6}$$

This equation is an expression of the initial axial pressure distribution for an infinitesimally short pulse duration. The pressure is proportional to the absorption coefficient and the fluence of the laser beam. For an

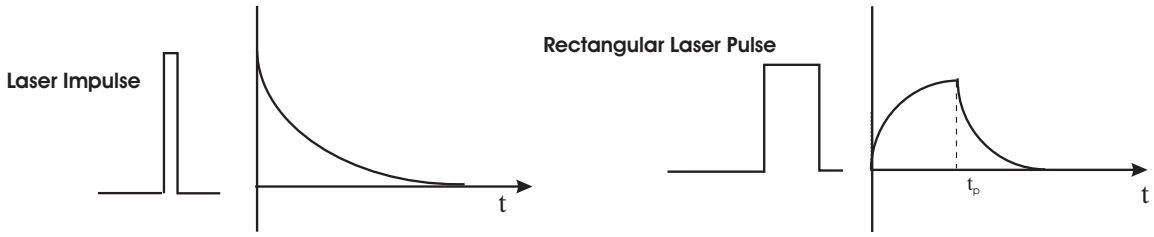

Figure 1. Photoacoustic signals for an impulse and a rectangular laser pulse.

infinitely large beam diameter, the temporal characteristics of the thermoelastic wave can be obtained from the initial pressure distribution simply by converting the axial distance z to time t using the speed of sound c.

To obtain the photoacoustic signal $P_L(t)$ for a pulse of finite duration, the laser pulse temporal profile $g(t)$ is convolved with the temporal extent of the impulsively generated initial pressure.[5]

$$P_L(t) = g(t) * p_0(t = \frac{z}{c}) \tag{7}$$

For $0 < t < t_p$, where t_p is the pulse duration:

$$P_L(t) = \frac{B\beta}{C\rho} F_0 \mu_a \frac{(1 - e^{(-\mu_a ct)})}{\mu_a ct} \tag{8}$$

For $t_p < t$:

$$P_L(t) = \frac{B\beta}{C\rho} F_0 \mu_a e^{(-\mu_a ct)} \frac{(e^{(-\mu_a ct_p)} - 1)}{\mu_a ct} \tag{9}$$

The peak pressure $P'_L(t)$ reaches its maximum when $t = t_p$ (see figure 1). Equation 8 can be rewritten thus

$$P'_L(t) = \frac{B\beta}{C\rho} F_0 \mu_a A \tag{10}$$

$$A = \frac{\left(1 - e^{(-\tau)}\right)}{\tau} \tag{11}$$

$$\tau = \frac{t_p}{t_s} = \mu_a c t_p \tag{12}$$

where A is termed the stress confinement coefficient[5,6] and t_s is the time for the thermoelastic wave to propagate across the source, known as the characteristic acoustic relaxation time.

To fulfil the stress confinement condition, the laser pulse duration has to be much shorter than the characteristic time of acoustic relaxation t_s.[5,7] If this condition is not respected, the photoacoustic signal will broaden and its peak amplitude will decrease. The stress confinement coefficient A provides a measure of this decrease in amplitude. As τ increases, the value of A will decrease to 0 and as τ decreases the values of A will increase to 1 (see figure 2.a). As the pulse duration increases, the fluence also increases assuming constant peak power. Therefore the peak pressure, defined by equation 10, will rise as the pulse duration increases before saturating at a maximum amplitude (see figure 2.b).

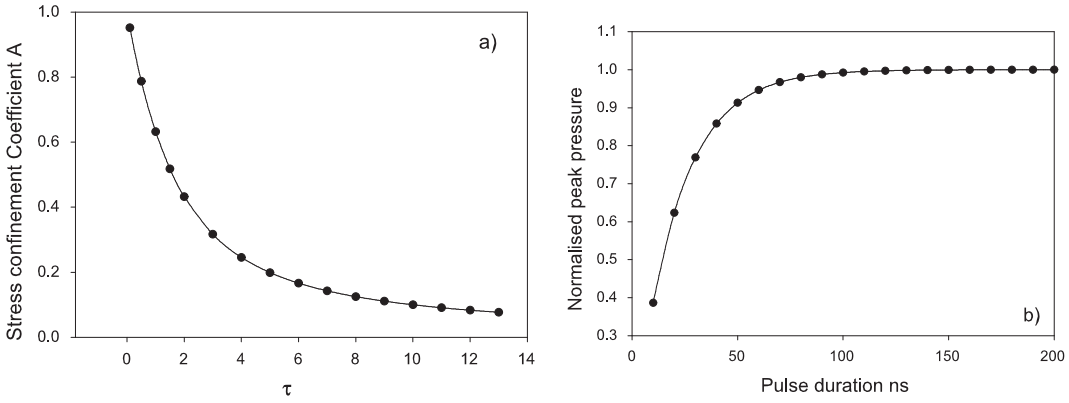

Figure 2. a) Stress confinement coefficient A. b) Normalised peak to peak amplitude, for constant power in a pure absorber ($\mu_a = 33\text{mm}^{-1}$).

2.2. Numerical model

In the previous section an analytical expression for the photoacoustic signal was developed for an impulse and a rectangular pulse of finite duration. Since this assumes a photoacoustic source of infinite lateral extent, it is problematic to validate experimentally. For this reason a numerical model which can simulate photoacoustic signals emitted by a source of finite lateral dimensions was also developed. This model is based on the Poisson solution to the wave equation[8–10] and uses an analytical expression of the initial pressure distribution.

$$\frac{\partial^2 p(r,t)}{\partial t^2} - c^2\nabla^2 p(r,t) = \frac{\partial}{\partial t} p_o(r)\partial(t) \tag{13}$$

$$p_0(r) = \frac{B\beta}{C\rho} F_0 \mu_a e^{-\mu_a z} f(x) \tag{14}$$

Where $f(x)$ is the lateral profile of the beam and x is the lateral dimension.

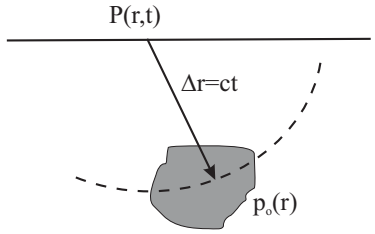

Figure 3. Numerical model.

The solution to equation 13 is

$$p(r,t) = \frac{1}{4\pi c}\frac{\partial}{\partial t}\left(\int \frac{p_o(r-\Delta r)}{ct} ds\right) \tag{15}$$

Where $p(r,t)$ is the acoustic pressure for an impulse and corresponds to the integration of the initial pressure distribution around the spherical shell s, given by $\Delta r = ct$ (see figure 3). The acoustic pressure $P_f(r,t)$ at the detector, for a finite pulse duration, is defined by the following convolution;

$$P_f(r,t) = g(t) * p(r,t) \tag{16}$$

This model also included the detector frequency response by averaging over the active volume of the detector.[10]

3. EXPERIMENTAL VALIDATION OF NUMERICAL MODEL

To validate the numerical model described in section 2.2, measurements of the photoacoustic signals excited in a pure absorbing medium were made.

3.1. Experimental Setup

A cylindrical cell filled with Indian ink was used as a source to generate photoacoustic waves. One side of the cell was composed of a perspex window to allow the ink to be illuminated by the laser beam. The other side of the cell was composed of a thin layer of cling film placed in contact with water (See figure 4.a). This piece of cling film was used for its acoustically transparent properties, allowing the photoacoustic signal generated in the ink cell to propagate into a water tank where a PVDF membrane hydrophone was placed. The illumination of the ink cell was achieved using a laser diode system, consisting of a pulsed laser dioder ($PGAF5S24$ from $EG\&G$) and a laser drive ($PCO-7120$ from DEI) which enabled the laser pulse duration to be varied. A 1.5mm core diameter multimode fibre was used to deliver the output of the laser to the cell. The beam diameter at the ink surface was 5mm. To detect the photoacoustic wave, it was necessary to amplifier the membrane hydrophone's output using a low noise voltage amplifier providing 40dB of gain (352A-1-B-1M, Analog Modules Inc.). The averaging and filtering modes of the Tektronix TDS-520 oscilloscope were also used to improve the detection of the signals, the bandwidth was limited to 20MHz and averaging over 200 signals was performed.

3.2. Measurements

Measurements of photoacoustic signals were made for different pulse durations and absorption coefficients. These measurements were compared to signals generated by the numerical model when using the same conditions. These signals correlated well with those provided by the model. Figure 4.b shows an example of these results where a 200ns pulse was used to generated a photoacoustic signal in a pure absorber (μ_a=33mm^{-1}), the differences between signals were due to noise.

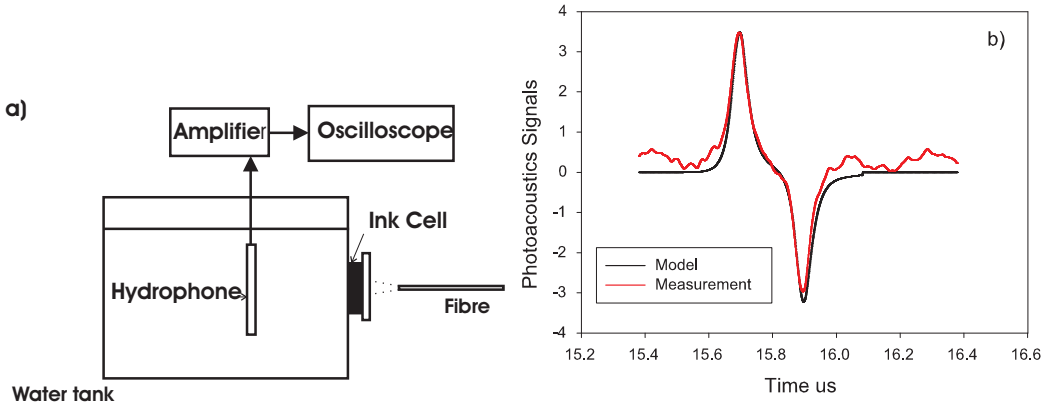

Figure 4. a) Experimental Setup. b) Photoacoustic signals generated by a 200ns pulse a in pure absorber (μ_a =33mm^{-1}) .

Measurements of the peak to peak amplitude of the photoacoustic signals were also made for the different absorbers and pulse durations. These measurements correlate well with the results provided by the numerical

model (See figure 5.a) and show the general behaviour seen in figure 2.b. The maximum peak amplitude was reached when the laser pulse duration was comparable to the time necessary for the acoustic wave to propagate across the source. Normalising all of these measurements with their respective pulse energy enabled the relative stress confinement coefficient A as a function of τ to be calculated (figure5.b). These values are in broad agreement with the theoretical plot in figure 2.a. This plot shows that for the high absorption coefficients the stress confinement condition was not fulfilled for long pulse duration.

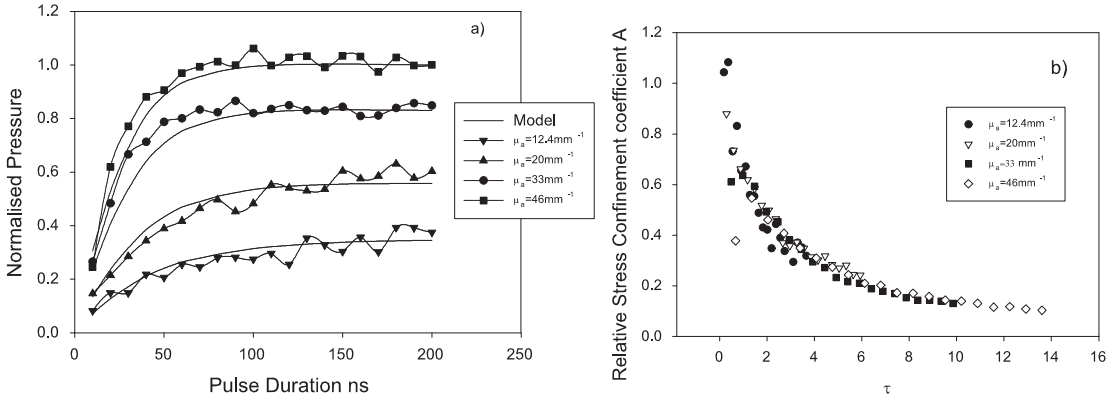

Figure 5. a) Normalised measurements of peak to peak pressure amplitude as a function of pulse duration. b) Measurements of the relative stress confinement coefficient A.

4. EFFECT OF PULSE DURATION

An aim of this study was to investigate whether it would be possible to generate photoacoustic signals more efficiently in tissue by optimising the pulse duration for specific depths in order to mitigate the effect of frequency dependent acoustic attenuation in tissue. For example, much of the higher frequency content of a photoacoustic signal generated at depth by the absorption of a short laser pulse may be lost due to acoustic attenuation. Under such circumstances it may be more efficient to deposit the laser energy over a longer pulse duration to preferentially excite a photoacoustic signal with a lower frequency content that will be attenuated less. However, as figure 2.a suggests, there is an opposing effect in that the efficiency of the generation process decreases with increasing pulse duration. To investigate the relative significance of these two processes and, in doing so, attempt to identify the optimum pulse duration as a function of depth, the numerical model described in section 2.2 was used to simulate the time domain acoustic signals produced by a planar absorber of thickness 10μm, positioned at various distances from the detector. To ensure that only plane waves were generated, the illuminating beam diameter was chosen to be sufficiently large that the plane and edge waves generated by the source were temporally distinct. The acoustic waveforms were then truncated in order to remove the edge wave contribution, Fourier Transformed to reveal their spectral content and the effect of the frequency dependent acoustic attenuation incorporated. An analysis based upon the total energy in the detected signal as a function pulse duration was then used to identify the optimum pulse duration regimes for two specific cases of interest: constant pulse energy and constant peak power.

4.1. Constant pulse energy

Figure 6 shows the acoustic frequency spectra of signals generated in the 10μm planar absorber when positioned at a depth of 1cm from the detector for pulse durations, t_P=10ns and t_P=200ns - the pulse energy is the same for both cases. Note that it is p^2 (where p is the acoustic pressure) that is plotted as a function of frequency since, for a plane wave, this is proportional to acoustic energy in the signal and it is this, as a proportion of the energy deposited into the target, that is of ultimate interest in this analysis. The spectra for the two pulse durations are shown with and without the effect of acoustic attenuation. It can be seen that the area

under the unattenuated spectrum (a measure of the total energy in the signal) for t_P=10ns is significantly larger than that for t_P=200ns. This is due to the more efficient sound generation that is achieved for short pulse durations - a manifestation of increasing stress confinement. When acoustic attenuation (assuming a figure of 0.6dB/cm/MHz)[11] is incorporated, the spectra for both pulse durations are significantly attenuated. For t_P=10ns, the decrease in the area under the spectrum as a proportion of the area under the corresponding unattenuated spectrum is greater than that for t_P=200ns. This is because the shorter pulse duration produces higher acoustic frequency components and these are more strongly attenuated. Despite this however, for t_P=10ns, the area under the attenuated spectrum is still significantly greater than for t_P=200ns because the higher generation efficiency achieved with the shorter pulse outweighs the losses due to acoustic attenuation for this depth and absorber dimensions. For these conditions it appears advantageous to operate at the shorter pulse duration.

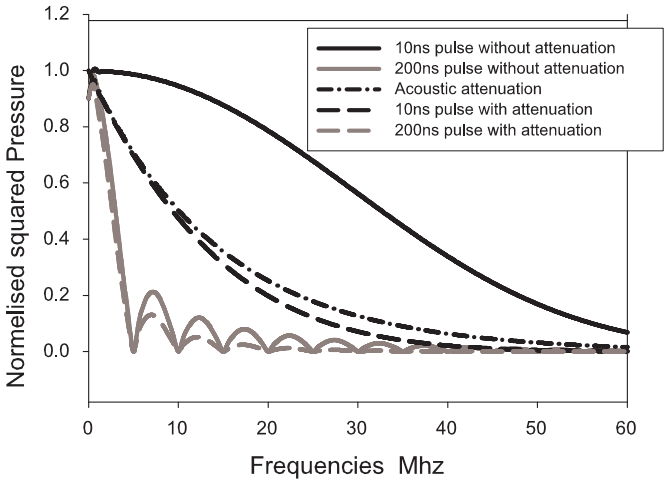

Figure 6. Frequency contents, with and without attenuation.

To investigate the above quantitatively, acoustic spectra were generated for a range of pulse durations and the effect of acoustic attenuation incorporated for 3 different absorber depths. As with the data in Figure 6, the laser pulse energy was held constant for all pulse durations. Figure 7.a shows the generation efficiency G_E, defined as the ratio of the energy in the photoacoustic signal generated with a finite pulse duration to that generated with a numerically simulated delta function - the energy being computed in both cases by integrating over the respective unattenuated p^2 frequency spectra. The fall-off in efficiency with increasing pulse duration is clearly in evidence. Figure 7.b shows the effect of acoustic attenuation alone by plotting R, the ratio of the energy in the attenuated photoacoustic signal to that in the unattenuated signal for depths of 1cm, 3cm and 5cm. It is evident that acoustic attenuation becomes less significant with increasing pulse duration as a greater proportion of the signal energy is shifted into lower frequencies which are attenuated less. Figure 7.c shows the product of G_E and R, thus combining the effects of acoustic attenuation and generation efficiency in order to provide a measure of the overall efficiency E_E.

For shorter depths, E_E falls off rapidly with increasing pulse duration because, with acoustic attenuation being relatively weak, the rapid decay in the generation efficiency G_E for small values of t_P (seen in Figure 7.a) dominates. As the depth of the absorber increases, acoustic attenuation becomes more significant. Thus for the 5cm depth, E_E is initially (up to $\sim$ 50ns) almost constant with pulse duration because, although G_E is decreasing rapidly, there is still sufficient energy in the high frequency region for acoustic attenuation to dominate. However for t_P >50ns, attenuation is reduced as the signal frequency content shifts to lower frequencies and the generation efficiency characteristics G_E now become significant and E_E begins to decrease. These results show that, given a hypothetical laser source that can provide pulses of constant energy with variable pulse durations, it is generally

desirable to employ short pulse durations for 1D source geometries. This is particularly so for superficial targets where acoustic attenuation is less significant and it is the generation efficiency characteristics that dominate.

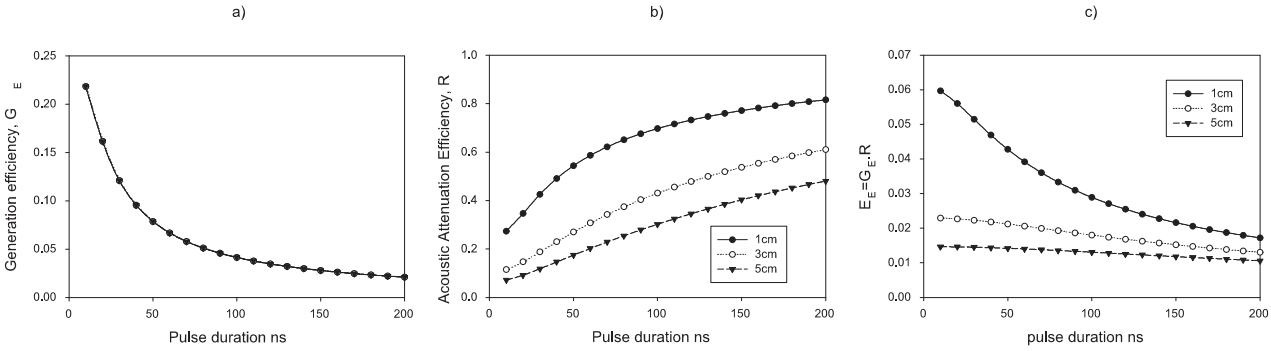

Figure 7. Effect of pulse duration for constant pulse energy. a)Generation efficiency G_E, b)acoustic attenuation R, c)$E_E = G_E.R$

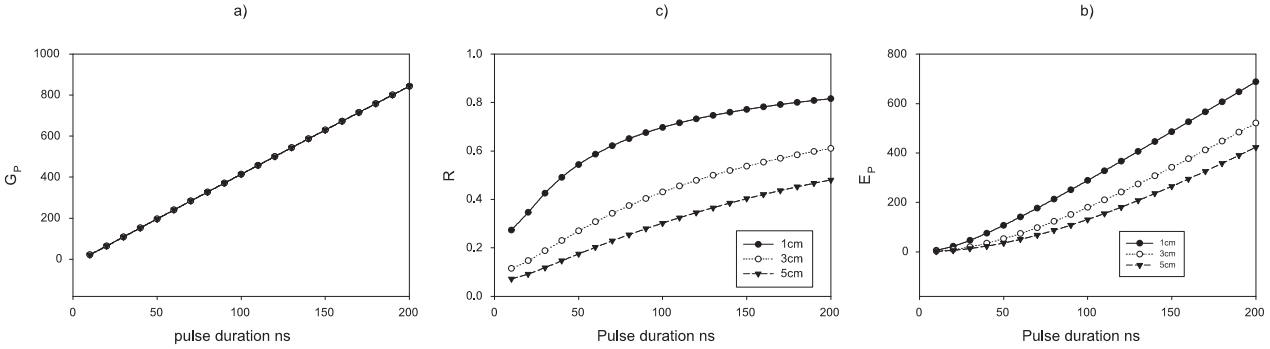

Figure 8. Effect of pulse duration for constant pulse power.

4.2. Constant peak power

The above analysis of photoacoustic signals as a function of pulse duration for constant pulse energy is useful in order to gain an insight into the underlying mechanisms. However, in order to determine the optimum pulse duration regime for a pulsed laser diode source, it is necessary to repeat the analysis with the peak power held constant as function of pulse duration. This new criterion is required because, in order to avoid facet damage, it is the maximum peak power that sets the operating limit of a laser diode operating at sub-μs pulse durations. The results for constant peak power are shown in figure 8. Note that although G_P is calculated in exactly same way as G_E in section 4.1 (ie the ratio of the energy in the photoacoustic signal generated with a finite pulse duration to that generated with a numerically simulated delta function) it is no longer strictly appropriate to denote it an"efficiency" term as, for constant peak power, the input energy increases with pulse duration. Figure 8(a) shows that G_P now increases linearly with t_P. When this is combined with the acoustic attenuation characteristics (figure 8(b)) to provide E_P (now a measure of the energy in the signal), shown in figure 8(c), it is clear that it is advantageous to operate at longer pulse durations. Note that this analysis is based on energy considerations alone. In practice other factors have to be taken into account. For example, although increasing the pulse duration will increase the total energy in the detected signal (for constant peak power), it will also progressively shift the signal energy to lower frequencies and therefore bandlimit the signal. Although this may be addressed in part (subject to SNR considerations) by deconvolving for the temporal profile of the laser pulse, there will inevitably be some loss of the higher frequency content of the signal. For applications that require

recovering spatial information from the time-domain photoacoustic signal this will reduce the achievable spatial resolution. One final point to be stressed is that, to provide an intuitively amenable description, the above analyses were undertaken for the specific case of a notional 1D geometry. It is expected that the optimum pulse duration regimes will be significantly different for the 2D and 3D source geometries characteristic of anatomically realistic targets. The analyses of these geometries will form the subject of future work in this area.

5. SIGNAL AVERAGING

It is suggested that the SNR of the photoacoustic signal could be significantly improved by exploiting the high repetition rate of the laser diode, to enable a large number of events to be acquired and signal averaged over a short period of time. The following analysis is based upon a comparison of the output of a laser diode source with the output of a Q - Switched Nd:YAG laser providing 10mJ pulses at a repetition rate of 20Hz - these output parameters are typical of those used to generate photoacoustic signals in tissue.

The SNR of a photoacoustic signal is directly proportional to the pulse energy of the laser when the stress confinement condition is satisfied. Therefore the ratio S of SNRs generated by the Q-switched laser and a laser diode, can be calculated from the ratio of energies of the laser pulses. Assuming a peak power of 175W at a pulse duration of 160ns for a single laser diode (PGA F5S24).

$$S = \frac{\text{pulse energy of Q} - \text{switched laser}}{\text{pulse energy of laser diode}} = \frac{10mJ}{160ns * 175Watts} = 357 \tag{17}$$

For this example the Q-switched laser pulse would produce a SNR that is 357 times greater than that generated by the laser diode, ignoring optical and acoustic attenuation and assuming stress confinement.

Consider the possible improvement on the ratio S when signal averaging is implemented over a period of 1 second. The repetition rate of the laser diode and the Q-switched laser are 5000Hz and 20Hz respectively. The laser diode repetition rate is limited by its duty cycle, typically 0.1% for a high peak power device. The improvement in SNR is directly proportional to square root of the number of events being averaged:

$$\frac{\text{Improvement in SNR } - \text{ laser diodes}}{\text{Improvement in SNR } - \text{ Q} - \text{switched laser}} = \frac{\sqrt{5000}}{\sqrt{20}} = 15.8 \tag{18}$$

This shows that by signal averaging over a period of 1 second the improvement in the laser diode SNR will be 15.8 times greater than that of the Q-switched laser, due to the much higher pusle repetition rate of the laser diode. The SNR of the Q-switched laser would then only be $\frac{357}{15.8} = 22.3$ times greater than that of the laser diode.

6. OPTICAL ATTENUATION

In the biomedical field photoacoustic signals are commonly generated using Nd:YAG lasers, operating at a wavelength of 1064nm. Light at this wavelength is relatively strongly attenuated by soft tissue, due to the water absorption peak at 940nm. Selecting a source with a wavelength that is attenuated less, would result in an improvement of the SNR of the photoacoustic signal.

At the depth at which the light becomes diffuse the axial fluence distribution in soft tissue can be approximated by

$$F(z) \propto F_0 e^{-\mu_{eff} z} \tag{19}$$

$$\mu_{eff} = \sqrt{(3\mu_a(\mu_a + \mu_s')} \tag{20}$$

where μ_{eff} is the effective attenuation coefficient, μ_a is the absorption coefficient and μ_s' is the reduced scattering coefficient, the latter is assumed to be relatively constant with wavelength in the NIR.

Equation 19 states that the fluence will decrease exponentially as a function of depth, at a rate dependent on the attenuation coefficients. In tissue the effective attenuation coefficient at 1064nm and 905nm are respectively $\mu_{eff} = 0.3\text{mm}^{-1}$ and $\mu_{eff} = 0.229\text{mm}^{-1}$.[12] Therefore the fluence for a source lasing at 1064nm will decrease with depth a greater rate than for a 905nm source. At a depth of 1cm the fluence delivered by a 905nm source would be twice that delivered by a 1064nm source for the same incident fluence.

7. CONCLUSION

This preliminary study showed that the low peak power of the laser diode could be overcome by exploiting the variable pulse length, the high repetition rate and the shorter wavelength of the laser diode. Section 5 showed that with signal averaging over second, the SNR produced by a 10mJ Q-switched laser pulse would only be 22.3 times greater than that generated by the laser diode. If the wavelength dependent optical attenuation in tissue is taken into account this result would be reduced by a factor of two, for a target at a depth of 1cm. This suggests that combining 12 laser diode would provide a SNR equivalent to a 10mJ Q-switched laser pulse, when the stress confinement condition is fulfilled. Therefore, by combining a reasonable number of laser diodes it should be possible to obtain adequate SNR for NIR spectroscopic photoacoustic applications.

ACKNOWLEDGMENTS

This work has been supported by the Engineering and Physical Sciences Research Council, UK

REFERENCES

1. Z. Zhao and R. Myllylä, "The effects of optical scattering on pulsed photoacoustic measurement in weakly absorbing liquids," *Measurement Science and Technology* **12**, pp. 2172–2177, 2001.
2. A. Duncan, J. Hannigan, S. S. Freeborn, P. W. H. Rae, B. McIver, F. Greig, E. M. Johnston, D. T. Binnie, and H. A. MacKenzie, "A portable non-invasive blood glucose monitor," *8th int. conf. on Solid-State Sensors and Actuators, and Eurosensors IX* **2**, pp. 455–458, 1995.
3. P. Hodgson, K. M. Quan, H. A. MacKenzie, S. S. Freeborn, J. Hannigan, E. M. Johnston, F. Greig, and T. Binnie, "Application of pulsed laser photoacoustic sensors in monitoring oil contamination in water," *Sensors and Actuators B* **29**, pp. 339–344, 1995.
4. J. Laufer, C. Elwell, D. Delpy, and P. Beard, "Pulsed near-infrared photoacoustic spectroscopy of blood," in *Photons Plus Ultrasound: Imaging and Sensing*, A. A. Oraevsky and L. V. Wang, eds., *Proc. SPIE* **5320**, pp. 57–68, 2004.
5. G. Paltauf, H. Schmidt-Kloiber, and M. Frenz, "Photomechanical processes and effecs in ablation," *Chem. Rev.* **103**, pp. 487–518, 2003.
6. R. S. Dingus and R. J. Scammon, "Grüneisen-stress induced ablation of biological tissue," in *Laser-Tissue Interaction II*, S. L. Jacques, ed., *Proc. SPIE* **1427**, pp. 45–54, 1991.
7. A. Vogel and V. Venugopalan, "Mechanisms of pulsed laser ablation of biological tissues," *Chem. Rev* **103**, pp. 577–644, 2003.
8. L. Landau and E. Lifshitz, *Fluid mechanics*, Butterworth Heinemann, Oxford, 1987.
9. G. Paltauf and P. E. Dyer, "Photoacoustic waves excited in liquids by fiber-transmitted laser pulses," *J. Acoust. Soc. Am.* **104**, pp. 890–897, 1998.
10. K. P. Köstli and P. C. Beard, "Two-dimensional photoacoustic imaging by use of fourier-transform image reconstruction and a detector with an anisotropic response.," *Applied Optics* **42**, pp. 1899–1908, 2003.
11. P. N. T. Wells, "Ultrasonic imaging of the human body," *Rep. Prog. Phys.* **62**, pp. 671–722, 1999.
12. G. M. Hale and M. R. Querry, "Optical constants of water in the 200 *nm* to 200 μm wavelength region," *Applied Optics* **12**, pp. 555–563, 1973.